Key Laboratory of Drug Targeting and Drug Delivery Systems, Ministry of Education, West China School of Pharmacy, Sichuan University, Sichuan, P. R. China

Intestinal absorption of raltitrexed and evaluation of the effects of absorption enhancers

YONG YU, YILING LU, XIANMEI ZHAO, XIAOSI LI, ZONGNING YIN

Received October 11, 2012, accepted February 17, 2012

Zongning Yin, Key Laboratory of Drug Targeting and Drug Delivery Systems, Ministry of Education West China School of Pharmacy, Sichuan University, Southern Renmin Road, No. 17, Section 3, Chengdu, 610041, P. R. China
yzn@scu.edu.cn

Pharmazie 68: 732–743 (2013) *doi: 10.1691/ph.2013.2828*

Raltitrexed (RTX) has shown clinical activity in a variety of advanced solid tumours. Its oral bioavailability is low and its intestinal absorption mechanism is not clear. In the present study, the absorption mechanism of RTX in the small intestine was investigated, and the effects of absorption enhancers and efflux transporter inhibitors were evaluated by *in vitro* transport studies using the Caco-2 cell model and *in situ* perfusion experiments in rats. Oral bioavailability of RTX in rats in the presence or absence of enhancers were also investigated. The results of *in vitro* and *in situ* experiments indicated that the kinetic model of combined mechanism (active and passive transport) fitted the concentration-time data of RTX best with the highest R^2 and lowest SSE (Sum of Squares for Error). The apparent or effective permeability coefficient (P_{app} or P_{eff}) of RTX remained statistically constant in a certain concentration range, then decreased when the concentration increased. But the decrease trend did not continue with further increase in concentration. And folic acid could competitively inhibit RTX absorption. These results suggested that a combined absorption mechanism for RTX existed. Furthermore, within certain concentration ranges, Carbomer 934P and sodium caprate (Cap-Na) exhibited significant absorption enhancement effects with low toxicity, whereas the enhancement effects of sodium deoxycholate (Deo-Na) were accompanied with acute toxicities. Moreover, probenecid and pantoprazole obviously enhanced RTX absorption, demonstrating that RTX is a substrate of the multidrug resistance protein (MRP) and breast cancer resistance protein (BCRP). A secretion experiment indicated that RTX could be effluxed into the intestines both with bile and by active efflux action. Oral bioavailability of RTX was significantly improved by the investigated absorption enhancers and transporter inhibitors, which is consistent with the *in vitro* and *in situ* experiments.

1. Introduction

Raltitrexed (RTX, ZD-1694) is a quinazoline folate analogue, which acts as a potent and specific inhibitor of thymidylate synthase (Van Vutsem et al. 2002). It has shown clinical activity in a variety of advanced solid tumours, such as colorectal cancer (Michels et al. 2006), head and neck cancer (Planting et al. 2005), malignant pleural mesothelioma (Woods et al. 2012) and non-small cell lung cancer (Manegold et al. 2002), both as a single agent and in combination with other compounds. The distribution, metabolism and excretion of RTX following intravenous administration have been extensively investigated in clinical and preclinical pharmacokinetic studies (Clarke et al. 2000). However, no research about the mechanism and influencing factors of intestinal absorption of RTX has been reported. Furthermore, the oral bioavailability of RTX in rats is only 10–20% (Jodrell et al. 1991), which greatly restricts oral administration.

The poor oral bioavailability of RTX is related to its chemical structure. Fig. 1 shows that RTX possesses a chemical structure similar to that of methotrexate (MTX), another folate analog (Wang et al. 2006), which is assigned as BCS (biopharmaceutical classification system) class III drug due to its high solubility and poor permeability (Lindenberg et al. 2004). Besides the permeability, the efflux transport mediated by ATP-binding cassette (ABC) transporter proteins including P-glycoprotein (P-gp), multidrug resistance protein (MRP) and breast cancer resistance protein (BCRP) (Leslie et al. 2005) may be factors responsible for the low oral bioavailability of RTX.

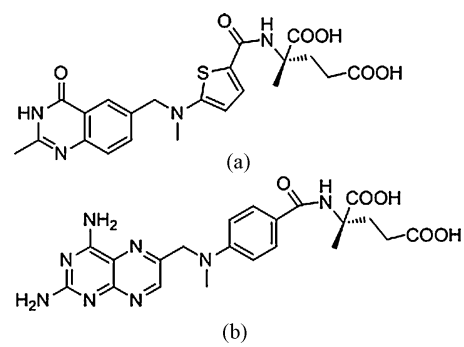

Fig. 1: Chemical structure of RTX (a) and MTX (b).

In order to improve the oral bioavailability of drugs with poor permeability, absorption enhancers have been often adopted to transiently increase permeation (Leone-Bay et al. 2000). In the

Table 1: Effects of folic acid and ABC transporter inhibitors on bi-directional transport of RTX in Caco-2 cell monolayer model (mean ± S, n = 3)

Group	$P_{app(AP\rightarrow BL)}$ (10^{-7}cm/s)	$P_{app(BL\rightarrow AP)}$ (10^{-7}cm/s)	Efflux ratio
control	0.67 ± 0.10	1.12 ± 0.07	1.82 ± 0.10
folic acid	0.38 ± 0.05*	0.71 ± 0.08*	1.87 ± 0.18
verapamil	0.70 ± 0.06	1.25 ± 0.19	1.79 ± 0.27
probenecid	2.37 ± 0.52*	2.04 ± 0.30*	0.86 ± 0.13*
pantoprazole	3.49 ± 0.92*	1.32 ± 0.16	0.38 ± 0.05*

*$P < 0.05$, compared to the control group.

present study, three different types of absorption enhancers with proven enhancement effects were selected, including sodium caprate (Cap-Na) (Maher et al. 2009; Mori at al. 2004), a fatty acid salt; sodium deoxycholate (Deo-Na) (Huang et al. 2006; Sharma et al. 2005), a bile acid salt; and Carbomer 934P (Thanou et al. 2001), a polyacrylate derivative. Their enhancement mechanisms have been related to promotion of transport through both transcellular and paracellular pathways. Research on the effects of these well-studied enhancers may provide supporting information for the investigation of absorption mechanisms for RTX. Moreover, application of efflux transporter inhibitors is another frequently-used strategy for oral bioavailability improvement. As extensively characterized inhibitors for P-gp, MRP and BCRP, verapamil (Bansal et al. 2009), probenecid (Zhou et al. 2010) and pantoprazole (Breedveld et al. 2006) are often co-administrated with drugs to improve the oral bioavailability and evaluate the role of P-gp and MRP in drug absorption.

The objectives of this study were to investigate the absorption and efflux mechanisms of RTX in the small intestine, and to evaluate the effects of absorption enhancers (Cap-Na, Deo-Na and Carbomer 934P) and efflux transporter inhibitors (verapamil, probenecid and pantoprazole) on the intestinal absorption of RTX. All the experiments were carried out *in vitro* using a Caco-2 cell monolayer model, rat *in situ* intestinal perfusion model and rat in vivo model.

2. Investigations and results

2.1. Bi-directional transport of RTX in Caco-2 cell monolayer model

The apical-to-bisolateral directional P_{app} values of RTX at various concentrations have been summarized and shown in Fig. 2A. The P_{app} values of RTX were quite low ($<10^{-7}$ cm/s) within the tested concentration range of 10–60 μg/mL, suggesting that RTX was poorly absorbed orally. When the RTX concentration was not more than 20 μg/mL, the P_{app} values showed no significant difference ($P > 0.05$). As the RTX concentration increased to 30 μg/mL, the P_{app} values obviously decreased to $0.35 \pm 0.06 \times 10^{-7}$ cm/s ($P < 0.05$). However, when the concentration continually increased to 45 and 60 μg/mL, the P_{app} values did not show significant decreases ($P > 0.05$).

In the basolateral-to-apical direction, the P_{app} value of RTX was $1.12 \pm 0.07 \times 10^{-7}$ cm/s (n = 3) at a concentration of 20 μg/mL. The efflux ratio ($P_{app(BL\rightarrow AP)}/P_{app(AP\rightarrow BL)}$) was 1.82, suggesting an efflux action during the RTX absorption.

2.2. Effects of folic acid and ABC transporter inhibitors on RTX transport in Caco-2 cell monolayer model

Table 1 shows the bilateral transport parameters of RTX with or without the addition of folic acid, verapamil, probenecid or pantoprazole. In comparison with the control group, addition

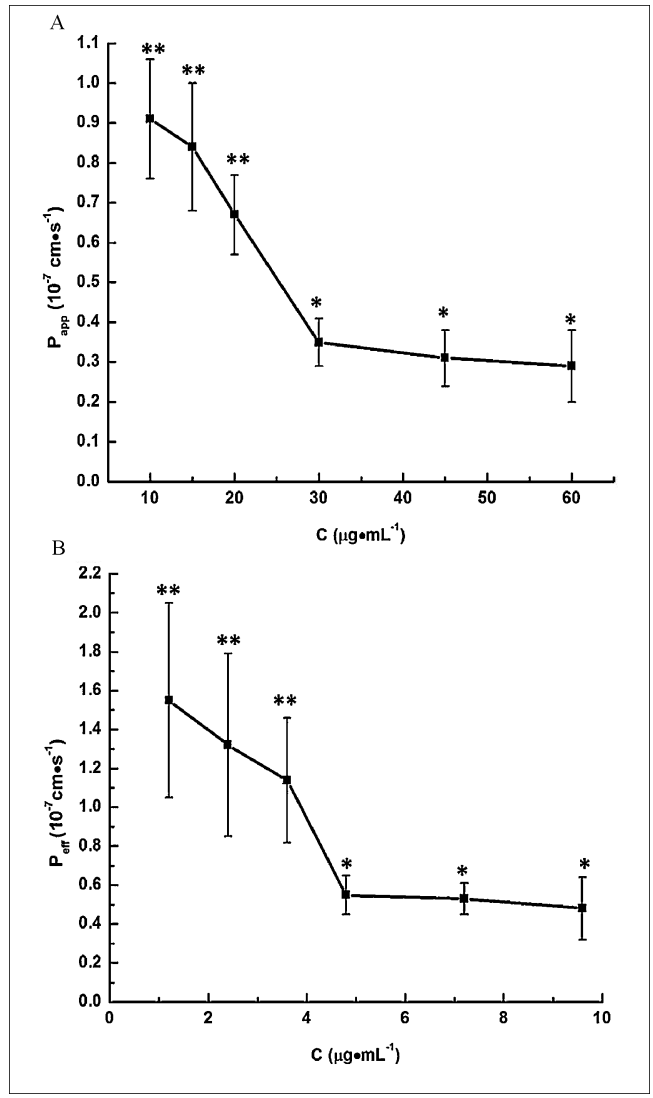

Fig. 2: Intestinal absorption of RTX at various concentrations *in vitro* and *in situ*. (A) Caco-2 cell monolayer model (n = 3), (B) *In situ* recirculating perfusion model (n = 5). *P < 0.05, compared to the group of 20 μg/mL (A) and 3.6 μg/mL (B); **P < 0.05, compared to the group of 30 μg/mL (A) and 4.8 μg/mL (B).

of folic acid resulted in a significant decrease in the bilateral P_{app} values of RTX. The verapamil group showed no significant difference in all parameters, while a significant increase in the apical-to-basolateral P_{app} value (3.54-fold, 5.21-fold) and a decrease in the efflux ratio (2.12-fold, 4.79-fold) were observed for the probenecid and pantoprazole group ($P < 0.05$), respectively. The results demonstrated that folic acid competitively inhibited RTX transport and RTX was a substrate of MRP and BCRP rather than P-gp.

2.3. Effects of absorption enhancers on the intestinal absorption of RTX in Caco-2 monolayer model

P_{app} value of RTX, without any enhancer, was set as the control, and the relative enhancement ratio was calculated as $P_{app(groups)}/P_{app(control)}$. In the presence of absorption enhancers, significant accumulation of RTX in the basolateral compartment caused notably higher P_{app} values ($P < 0.05$). As shown in Table 2, the P_{app} values of RTX increased in a concentration-dependent manner for all the three enhancers within the tested concentration ranges (Cap-Na: 0.1%–0.5% w/v, Deo-Na: 0.025%–0.25% w/v, Carbomer 934P: 0.1%–1% w/v). The

Table 2: Permeation enhancing effects of Cap-Na, Deo-Na and Carbomer 934P on the transport of RTX and related toxic values in Caco-2 cell monolayer model (mean ± S, n = 3)

Group	Papp (10^{-7} cm/s)	Enhancement ratio	$TEER_{3h}$ (%)	$TEER_{24h\ post}$ (%)	Protein-release amount(mg/mL)	Viability rate (%)
HBSS	-	-	87.65 ± 4.79	90.20 ± 5.65	0.0565 ± 0.0058	100%
RTX	0.35 ± 0.06	1	88.52 ± 11.31	89.49 ± 12.89	0.0579 ± 0.0063	102.47 ± 4.80
Cap-Na						
0.1%	1.86 ± 0.43	5.32	45.54 ± 2.05	81.82 ± 4.34	0.0546 ± 0.0077	104.84 ± 14.56
0.125%	18.23 ± 4.20	52.00	13.10 ± 0.81	80.94 ± 7.60	0.0613 ± 0.0121	90.43 ± 9.74
0.15%	54.60 ± 5.11	155.75	4.88 ± 0.61	34.64 ± 12.50	0.1320 ± 0.0123	7.29 ± 0.80
0.25%	76.44 ± 9.12	218.04	5.01 ± 0.75	1.18 ± 0.13	0.1415 ± 0.0153	6.80 ± 0.77
0.5%	86.39 ± 6.29	246.42	4.09 ± 1.17	1.10 ± 0.35	0.1525 ± 0.0117	6.31 ± 0.45
Deo-Na						
0.025%	3.60 ± 0.53	10.28	25.10 ± 3.23	64.52 ± 4.80	0.0899 ± 0.0048	23.38 ± 4.28
0.05%	3.76 ± 0.21	10.72	27.32 ± 1.95	69.47 ± 4.71	0.0964 ± 0.0120	10.99 ± 0.66
0.075%	36.88 ± 3.71	105.21	14.92 ± 2.11	41.54 ± 9.64	0.2110 ± 0.0489	5.30 ± 1.43
0.1%	65.81 ± 8.73	187.73	4.62 ± 0.24	13.49 ± 1.27	0.4889 ± 0.0537	3.00 ± 0.53
0.25%	74.53 ± ± 5.26	212.60	3.03±1.23	2.10 ± 0.33	0.5813 ± 0.0650	1.58 ± 1.10
Carbomer 934P						
0.1%	1.05 ± 0.24	3.00	90.39 ± 13.09	93.22 ± ± 8.94	0.0575 ± 0.0104	105.45 ± 10.46
0.25%	7.75 ± 1.20	22.10	76.28 ± 0.63	85.67 ± 8.55	0.0637 ± 0.0054	99.92 ± 5.85
0.5%	11.29 ± 1.24	32.21	12.65 ± 2.97	81.32 ± 7.89	0.0706 ± 0.0164	61.23 ± 7.14
0.75%	20.16 ± 3.58	57.53	14.96 ± 2.61	14.82 ± 2.68	0.0711 ± 0.0059	29.17 ± 1.63
1%	35.21 ± 2.87	100.43	16.34 ± 3.19	5.48 ± 0.94	0.0941 ± 0.0015	13.63 ± 0.13

absorption enhancement effect among the three enhancers could be ranked as Deo-Na > Cap-Na > Carbomer 934P.

2.4. Toxic effects of absorption enhancers on Caco-2 cell monolayers

2.4.1. TEER measurement

As shown in Table 2, the increase in P_{app} values was accompanied with a decrease of TEER values, indicating the opening of tight junctions. Also, TEER values were measured after 24 h recovery from the effects of enhancers. The data demonstrated that TEER values were restored to > 80% after recovery for monolayers treated with 0.1%, 0.125% (w/v) Cap-Na and 0.1%, 0.25%, 0.5% (w/v) Carbomer 934P, suggesting good reversibility of their effects on monolayers. All the three enhancers at other concentrations exhibited permanent damage to the cells with irreversible decreased TEER values. The result indicated that the enhancement effects of Cap-Na and Carbomer 934P at proper concentrations were due to reversible opening rather than loss of intercellular tight junctions.

2.4.2. Protein-release measurement

Perturbation of membrane by absorption enhancers results in the release of proteins from enterocytes into lumen, and the extent of protein-release is considered as a direct measure of cytolytic potential of compounds (Gao et al. 2008; Hamid et al. 2009). Therefore, the amount of protein released from cell monolayers can be employed as an indication of toxic effects of absorption enhancers toward Caco-2 cells. Table 2 shows that Cap-Na at concentrations of 0.1%, 0.125% (w/v) and Carbomer 934P at all tested concentrations except 1% (w/v) exhibited low toxicity compared with the negative control ($P > 0.05$). Deo-Na presented obvious toxic effects on membrane even at a concentration of 0.025% (w/v). The membrane toxicity toward Caco-2 cells among the three enhancers could be ranked as Deo-Na > Cap-Na > Carbomer 934P.

2.4.3. Cytotoxicity measurement

As summarized in Table 2, Cap-Na (0.1%, 0.125% w/v) and Carbomer 934P (0.1%, 0.25% w/v) exhibited total safety to Caco-2 cells with cell viability rate of > 90%. However, Deo-Na showed obvious cytotoxicity toward Caco-2 cells even at an extremely low concentration (0.025% w/v) with a cell viability of 23.38 ± 4.28%. A concentration dependent increase in the cytotoxicities was seen among all the three enhancers in the tested ranges of concentration.

2.5. Intestinal absorption of RTX in rat in situ recirculating perfusion model

Fig. 2B shows the variation trend of P_{eff} values for RTX at various concentrations. The P_{eff} values were quite low ($<10^{-6}$ cm/s), which could explain the poor oral bioavailability of RTX. Data demonstrated that higher RTX concentration resulted in lower P_{eff}. Moreover, no statistically significant differences were observed among P_{eff} values ($P > 0.05$) within the RTX concentration range of 1.2–3.6 μg/mL. When the RTX concentration increased to 4.80 μg/mL, P_{eff} showed apparent decrease ($P < 0.05$). However, the P_{eff} of RTX at 4.80 μg/mL was not significantly different from that of RTX at 7.2 and 9.60 μg/mL ($P > 0.05$).

2.6. Effects of folic acid and ABC transporter inhibitors on intestinal absorption of RTX in rat in situ recirculating perfusion model

Table 3 lists the P_{eff} values for RTX with or without the addition of folic acid, verapamil, probenecid and pantoprazole. With the addition of folic acid, P_{eff} values of decreased obviously comparing with the control group ($P < 0.05$). And no statistically significant difference of P_{eff} values was observed ($P > 0.05$) between the verapamil group and control group. In contrast, the probenecid group and pantoprazole group displayed significantly enhanced P_{eff} values ($P < 0.05$). The results indicated that

Table 3: Effects of folic acid and ABC transporter inhibitors on intestinal absorption of RTX in rat in situ perfusion model (mean ± S, n = 5)

Group	control	folic acid	verapamil	probennecid	pantoprazole
$P_{eff} \times 10^{-7}$ (cm·s^{-1})	1.14 ± 0.32	0.65 ± 0.18*	1.62 ± 0.80	2.02 ± 0.22*	2.15 ± 0.30*

* $P < 0.05$, compared to control group.

folic acid was the competitive inhibitor for RTX absorption and RTX could be effluxed by MRP and BCRP in the intestine.

2.7. Secretion of RTX from in situ intestine segment

The P_{eff} values of RTX for secretion were 53.57 ± 4.38 cm·s^{-1} for the control group and 13.54 ± 1.61 cm·s^{-1} for the bile duct ligation group, respectively (n = 5). And the RTX concentration in the perfusion solution began to increase at 15 min after the RTX injection in both groups. The results indicated that RTX could be serected into the *in situ* intestine segment in both groups, and the serection parameters of the bile duct ligation group were obviously higher than those of the control group.

2.8. Effects of absorption enhancers on the intestinal absorption of RTX in rat in

As shown in Fig. 3, the addition of Cap-Na, Deo-Na and Carbomer 934P (0.25–1% w/v) resulted in significantly increased P_{eff} values by 2.32–2.70-fold, 1.81–2.61-fold and 2.34–4.13-fold, respectively. And the P_{eff} value of RTX increased in a concentration-dependent manner for all the three absorption enhancers. The absorption enhancement effect among the three enhancers could be ranked as Carbomer 934P > Cap-Na > Deo-Na.

2.9. Epithelial toxicities of absorption enhancers on the intestinal segments

2.9.1. Protein-release measurement

Fig. 4 shows that the amount of protein released from epithelium treated with Carbomer 934P at all tested concentrations and Cap-Na at the concentration of 0.25% (w/v) was not significantly different from that of the negative control ($P > 0.05$). Deo-Na at all tested concentrations and Cap-Na at other concentrations presented evident epithelial toxicities. Cap-Na and Deo-Na increased the amount of released protein in a concentration-dependent manner. The epithelial toxicities among the three enhancers could be ranked as Deo-Na > Cap-Na > Carbomer 934P.

2.9.2. Histological evaluation of intestinal segments

Fig. 5 shows that NPA of enterocytes and Vi of villus decreased in the presence of all the three enhancers, while increases of morphological scoring were observed. Both Cap-Na and Carbomer 934P at concentrations of 0.25% and 0.5% (w/v) exhibited low toxicities with slight decrease of NPA, Vi and morphological scorings of no more than 2. All the three enhancers at other concentrations showed obvious epithelial toxicity ($P < 0.05$). Photomicrographs of duodenum were selected to display the morphological changes of intestine (Fig. 6).

2.10. Fitting of kinetic models to concentration-time data of RTX

The indexes of goodness of fit for the three kinetic models are listed in Table 4. In the comparison with the other two models, the model of combined mechanism (active and passive transport) provided the best fit with the highest R^2 (0.9040 for *in vitro* and 0.9172 for *in situ*) and the lowest SSE (0.02071 for *in vitro* and 0.00056 for *in situ*). So the absorption process of RTX in intestine should be described as a combined mechanism involving both active and passive transport.

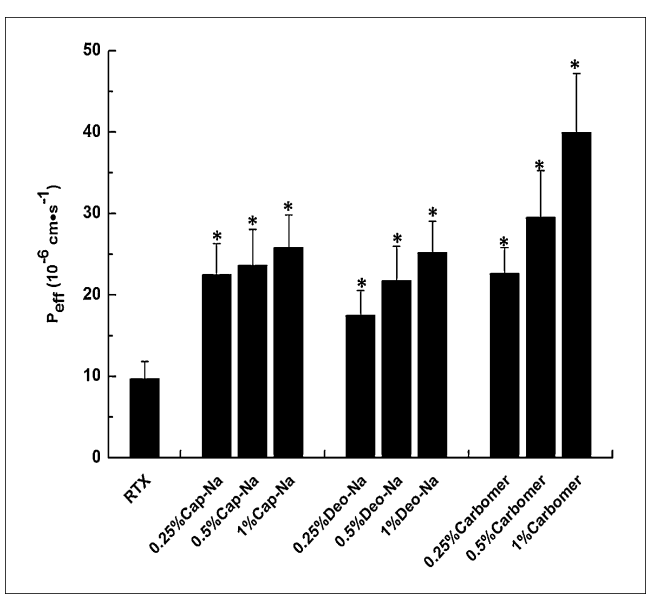

Fig. 3: Permeation enhancing effects of Cap-Na, Deo-Na and Carbomer 934P on the intestinal absorption of RTX in rat *in situ* single-pass perfusion model, n = 5. *P < 0.05, compared to the RTX group.

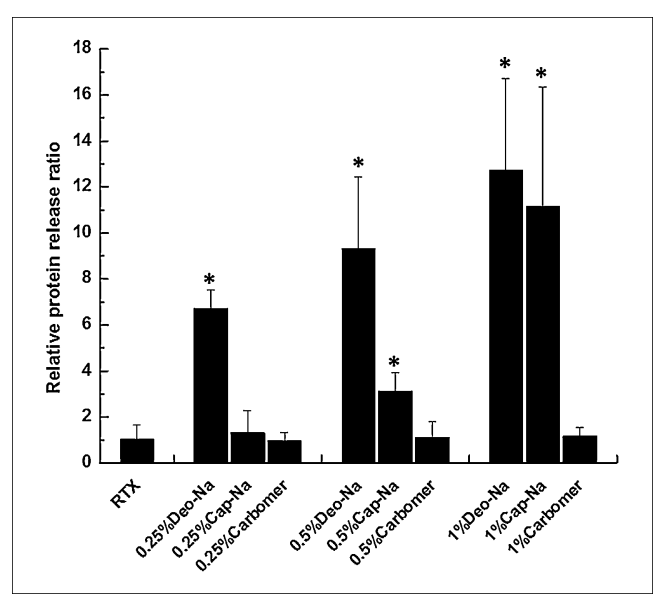

Fig. 4: Comparison of epithelium toxicity among Cap-Na, Deo-Na and Carbomer 934 in rat *in situ* intestinal perfusion model, n = 5. *P < 0.05, compared to the RTX group.

Table 4: Evaluation of fit goodness for the three kinetic model to the concentration-time data of RTX obtained from *in vitro* and *in situ* experiments

Index	*In vitro*		*In situ*	
	R^2	SSE	R^2	SSE
Passive transport	−2.724	0.8032	−1.1	0.01408
Active transport	0.8891	0.02393	0.9023	0.00066
Combined mechanism	0.9040	0.02071	0.9172	0.00056

2.11. Effects of absorption enhancers and ABC transporter inhibitors on oral bioavailability of RTX in rats

As shown in Table 5, the plasma C_{max} and $AUC_{0\text{-}24}$ of RTX in the presence of all tested enhancers and transporter inhibitors following oral administration in rats were significantly improved in comparison with the control group. And the enhancement effects of the three enhancers were consistent with the concentration-dependent manner mentioned in the *in vitro* and *in situ* experiments. T_{max} of RTX was significantly postponed with the addition of Carbomer 934P at all the tested concentrations. Plasma concentration-time profiles of the selected enhancers with low toxicities toward intestinal epithelium were plotted in Fig. 7.

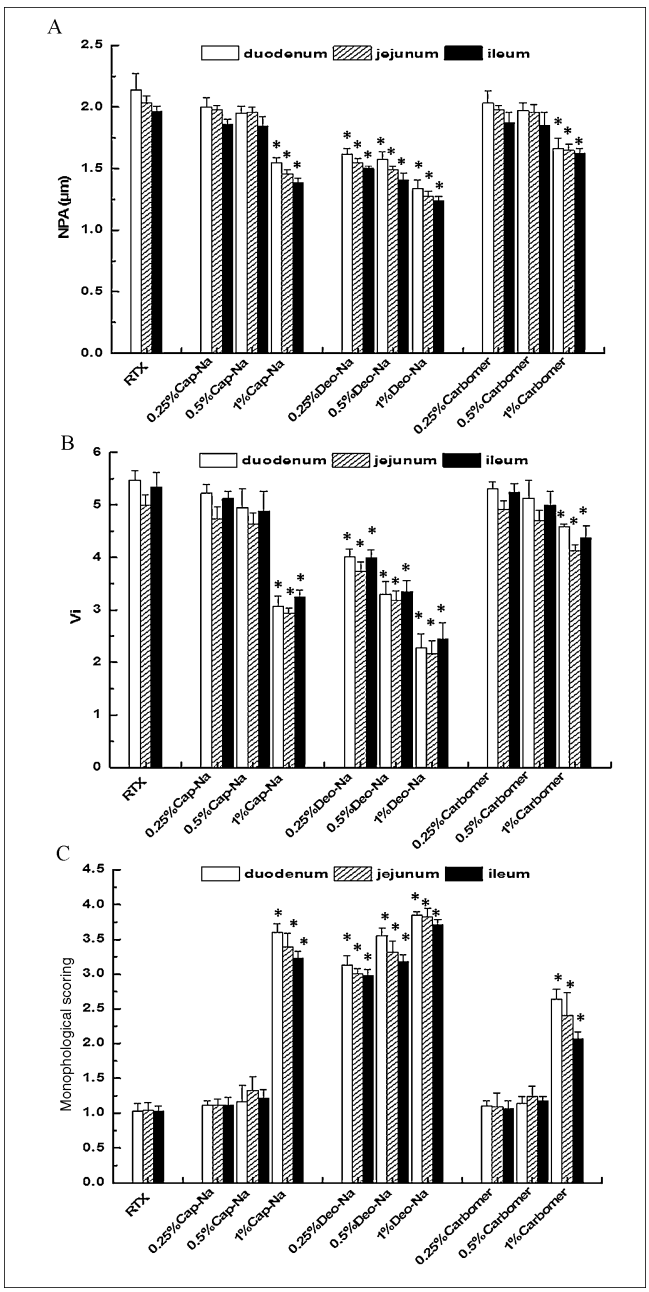

Fig. 5: Morphological parameters of different intestinal segments of rat after *in situ* perfusion experiments with absorption enhancers, n = 5. (A) NPA, (B) Vi, (C) Morphological scoring. *P < 0.05, compared to the RTX group.

3. Discussion

3.1. Adoption of in situ perfusion models

In the present study, two different *in situ* perfusion models were adopted for different research purposes: the recirculating model for absorption mechanism study and the single-pass model for absorption enhancers investigation. The adoptions were based on the different means of volume correction in the two models: addition of non-absorbable marker for recirculating model (Li et al. 2009; Zhou et al. 2010) and gravimetric measurement for single-pass mode (Jonker et al. 2002; Li et al. 2011). Since the non-absorbable marker may be absorbed in the presence of absorption enhancers (Nakamura et al. 1979), the recirculating perfusion model is not adaptable for the study of absorption enhancers. However, the single-pass perfusion model may be unsuitable in the investigation of absorption mechanism due to its constant drug concentration of influent perfusate, which does not exist in the actual process of intestinal drug absorption.

Table 5: Pharmacokinetic Parameters of RTX after oral administration in rats in the presence or absence of absorption enhancers (mean ± S, n = 5)

Group	C_{max} (μg/mL)	Tmax (h)	$AUC_{0\text{-}24}$ (μg·mL^{-1}·h)
control	1.56 ± 0.17	2.00 ± 0.02	16.74 ± 1.48
Cap-Na			
0.25%	1.82 ± 0.11*	2.00 ± 0.05	21.00 ± 1.95*
0.5%	2.53 ± 0.20*	2.05 ± 0.12	24.40 ± 1.86*
1%	2.86 ± 0.26*	2.11 ± 0.18	26.47 ± 2.38*
Deo-Na			
0.25%	1.72 ± 0.16*	1.98 ± 0.13	19.49 ± 1.79*
0.5%	2.01 ± 0.20*	2.03 ± 0.06	21.03 ± 1.73*
1%	2.20 ± 0.27*	2.09 ± 0.20	22.93 ± 2.38*
Carbomer 934P			
0.25%	2.27 ± 0.23*	2.52 ± 0.41*	23.40 ± 2.17*
0.5%	2.93 ± 0.30*	2.93 ± 0.18*	27.58 ± 2.08*
1%	3.17 ± 0.28*	3.04 ± 0.14*	32.27 ± 3.25*
probennecid	1.65 ± 0.18*	2.02 ± 0.09	19.03 ± 1.68*
pantoprazole	1.72 ± 0.17*	2.07 ± 0.10	20.26 ± 1.59*

* $P < 0.05$, compared to the control group.

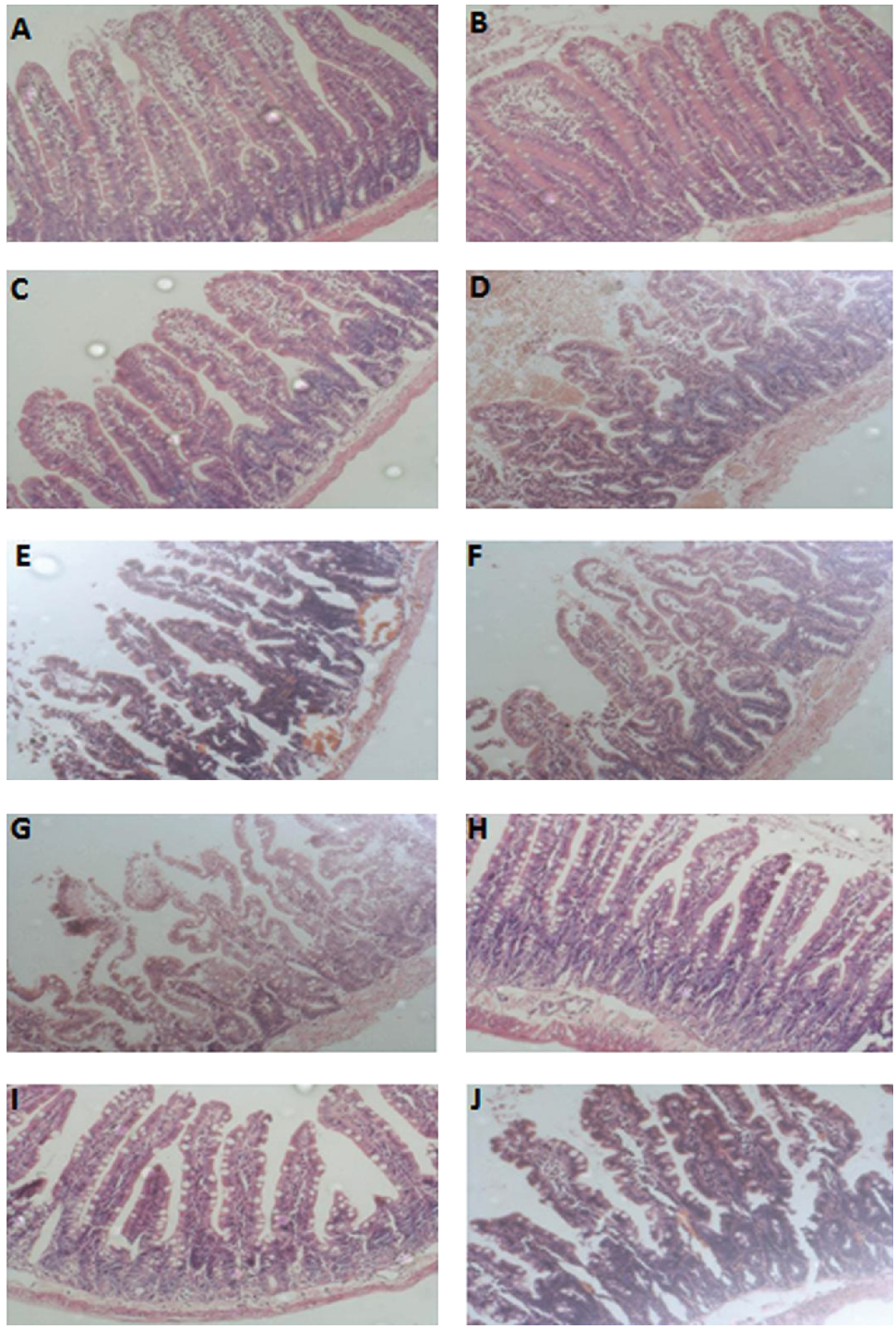

Fig. 6: Representative photomicrographs (×200) of duodenal segment of rat after *in situ* perfusion experiments with absorption enhancers. (A) Control, (B) 0.25% Cap-Na, (C) 0.5% Cap-Na, (D) 1.0% Cap-Na, (E) 0.25% Deo-Na, (F) 0.5% Deo-Na, (G) 1.0% Deo-Na, (H) 0.25% Carbomer 934P, (I) 0.5% Carbomer 934P, (J) 1.0% Carbomer 934P (w/v, Bar = 50um).

3.2. Intestinal absorption mechanism of RTX

P_{app} and P_{eff} are absorption parameters that are usually calculated to describe the absorption behavior of drugs and reflect the absorption mechanism (Lennernas 1998; Yasuno et al. 2012; Zhou et al. 2010). In the present study, the *in situ* investigation of RTX absorption at six different concentrations indicated that as the RTX concentration increased, P_{eff} values decreased and there was a saturable process, suggesting a carrier-mediated transport mechanism. And the absorption process could be competitively inhibited by folic acid. So RTX and folic acid might share the same transport system. This was consistent with the reported transport mechanism of MTX (Cercos-Fortea et al. 1997). Because the quantity of carrier was limited and invariable, at low concentrations, the absorption rate was positively correlated with drug concentration and P_{eff} was a theoretical constant. However, when the transport was saturated, the absorption rate stopped increasing, and P_{eff} began to decrease with further increase of drug concentration. Statistical analysis showed that there was no statistically significant difference among the P_{eff} values ($P > 0.05$) within the concentration range of 1.2–3.6 μg/mL. When the RTX concentration increased to 4.80 μg/mL, P_{eff} decreased significantly ($P < 0.05$). However, the P_{eff} of RTX at 4.80 μg/mL did not significantly differ from that of 7.2 and 9.60 μg/mL ($P > 0.05$), which demonstrated that another transport mechanism may also contribute to RTX

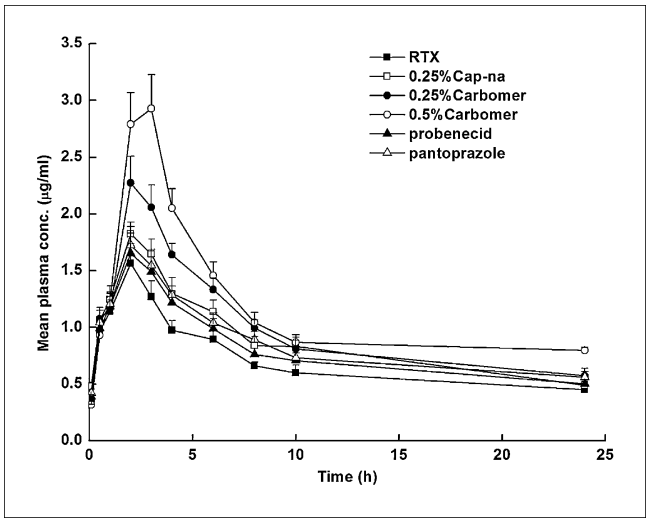

Fig. 7: Plasma concentration-time profiles of RTX in the presence or absence of selected enhancers after oral administration in rats, n = 5.

absorption. Similar results were obtained from the *in vitro* transport experiment through the Caco-2 cell monolayer model. The P_{app} values remained basically stable ($P > 0.05$) within the concentration range of 10–20 μg/mL and then an obvious decrease ($P < 0.05$) appeared at a concentration of 30 μg/mL. But when the concentration was raised to 45 and 60 μg/mL, no significant difference of P_{app} values was observed ($P > 0.05$). According to the chemical structure, RTX is partly of ionic state at physiological pH, so it also can be absorbed through paracellular pathways. Therefore, passive transport can not be excluded, and the intestinal absorption of RTX should be considered as a combined mechanism. Besides, according to the results of Nonlinear Curve Fit process, the combined mechanism model (active and passive transport) provided the best fit to the concentration-time data of RTX obtained from *in vitro* and *in situ* experiments with the highest R^2 and lowest SSE, which demonstrated the existence of a combined mechanism during the intestinal absorption of RTX. In summary, the whole absorption process could be described as: active transport played the major role when the carriers were undersaturated; after the saturation of carriers, passive transport through the paracellular pathways would take the dominant position with the RTX concentration increasing; the K_a values for passive transport were significantly lower than those for active transport.

3.3. Efflux behavior of RTX in intestine

A drug can be secreted into intestine with bile or by active efflux action. The comparison of bilateral P_{app} values of RTX in Caco-2 cell monolayer model showed that the efflux ratio was 1.82, suggesting an efflux action during the RTX transport. During the rat *in situ* perfusion experiment, RTX could be detected in perfusate 15 min after the injection with or without bile duct ligation. And the accumulation of secreted RTX in the bile duct ligation group was less than that in the control group. The results demonstrated that RTX could be secreted into the intestine both with bile and by other efflux routes, which could contribute to the low bioavailability. Furthermore, evaluation of the effect of verapamil on RTX absorption exhibited negative results. In contrast, probenecid and pantoprazole enhanced the RTX transport in apical-to-basolateral direction significantly both *in vitro* and *in situ*, and the oral bioavailability of RTX was obviously improved in the presence of probenecid and pantoprazole (Fig. 7). These results indicated that the efflux action for RTX in intestine was mediated by MRP and BCRP. This is consistent with the reported efflux mechanism for antifolates (Assaraf 2006).

3.4. Investigation of absorption enhancers

Since cell culture models are usually more sensitive to absorption enhancers than intact intestine membranes (Zhou et al. 2009), both the absorption enhancement effects and toxic effects of enhancers on the Caco-2 cell monolayers were much more obvious than those on *in situ* intestinal segments in this study. These differences could be due to the existence of a protective mucous layer acting as a diffusion barrier in the intact intestine. Moreover, the intact tissue has mechanisms of recovery from trauma, which may not be present in cell cultures (Aùngst 2000). Our data showed that Deo-Na and Cap-Na exhibited significantly different absorption enhancement effects between the *in vitro* and *in situ* models. The relative enhancement ratios of the two enhancers were no more than 3-fold in the *in situ* perfusion model even when their concentration was as high as 1% (w/v). In contrast, the ratios of Deo-Na and Cap-Na at lower concentration (0.25% and 0.5% w/v, respectively) acquired from the *in vitro* transport experiment became more than 200-fold. Interestingly, this type of variance for Carbomer 934P between the two models was not as huge as with the other two enhancers. It could be explained by different action mechanisms of absorption enhancers. As a mucoadhesive polymer, Carbomer 934P is thought to interpenetrate the mucous layer, thus reaching the physical barrier and facilitating transport of hydrophilic molecules across the mucous layer (Lehr et al. 1992; Pitelka et al. 1983). Its enhancement mechanism is probably a combination of mucoadhesive properties and influence on the intercellular tight junctions (Luessen et al. 1996). The opening of the tight junctions is realized by removing the endogenous Ca^{2+} from the intestinal epithelial cells through the formation of poly(acrylic acid)-Ca^{2+} complexes (Junginger and Verhoef 1998). The mild mechanism determines its low membrane toxicity, which is consistent with the results of protein-release measurement in this study. However, due to the high viscosity and adhesive character, not all of the polymer solutions can be removed without damaging the cells (Borchard et al. 1996), which could explain the relatively high cytotoxicity at concentrations of more than 0.5% (w/v).

Previous studies have suggested that the absorption enhancement effects of Deo-Na and Cap-Na are implemented through both the transcellular and paracellular routes (Lo and Huang 2000). With a high capacity for phospholipid solubilization (Aùngst. 2000), Deo-Na promotes the absorption mainly through removing phospholipids from cell membrane components, solublizing the cell membrane to facilitate transcellular transport and interacting with Ca^{2+} to loosen intercellular tight junctions (LeCluyse and Sutton 1997; Lin and Shen 1991; Sharma et al. 2005). Membrane solublization has been observed as the major mechanism, and the breakdown of membrane structure may result in the release of proteins and phospholipids, leading to the damage to the intestinal mucosa. This mechanism could explain its significant enhancement effects in cell model and extremely high toxic effects *in vitro* and *in situ* in this study. As one of the most extensively used absorption enhancers, Cap-Na has been studied for years, and its action mechanism has also been thoroughly investigated. It acts on both the paracellular and transcellular pathways. The promotion of paracellular transport is modulated by opening intercellular tight junctions through interactions with Ca^{2+} (Kurasawa et al. 2009; Sugibayashi et al. 2009). For transcellular permeation, Cap-Na can also partition into lipid bilayers to disrupt intermolecular forces

between membrane phospholipids and even result in destabilization and solubilisation of enterocyte membranes (Tomita et al. 1988, 1992). Modulation of paracellular transport plays the major role at low concentrations, the contribution of transcellular permeation pathways may be improved with the increase of concentration. Therefore, proper concentrations always exist, at which Cap-Na may present significant absorption enhancement effect with low toxicity. In our study, 0.25% (w/v) was the proper concentration for *in situ* perfusion experiment, and 0.1% and 0.125% (w/v) were the proper concentrations for *in vitro* experiment.

In addition, the insignificant effect of verapamil on RTX transport excluded the possible existence of inhibition of P-gp from the enhancement mechanism of all three enhancers. Moreover, the conspicuous effects of Carbomer 934P on RTX absorption both *in vitro* and *in situ* supported the point that transport through paracellular routes was a part of the combined mechanism of RTX transport.

The oral bioavailability study in rats indicated that the investigated enhancers (Cap-Na, Deo-Na and Carbomer 934P) and transporter inhibitors (probenecid and pantoprazole) promoted the absorption of RTX significantly with increased C_{max} and $AUC_{0\text{-}24}$. These results were consistent with those of *in vitro* and *in situ* experiments. Besides, an significantly postponed T_{max} of RTX in the presence of Carbomer 934P suggested that a sustained release process may exist during the absorption of RTX due to the swelling properties of Carbomer 934P (Wang and Tang. 2008).

Taken together, the intestinal absorption of RTX was realized through a combined mechanism, involving active transport mediated by carriers and passive transport through paracellular routes. RTX was a substrate of MRP and BCRP. It could be effluxed into the intestine both with bile and through active efflux. Furthermore, within certain concentration ranges, Carbomer 934P and Cap-Na had significant enhancement effects on RTX absorption with low toxic effects both *in vitro* and *in situ*, whereas the enhancement effects of Deo-Na were accompanied with acute toxicities. So probenecid, pantoprazole, Cap-Na and Carbomer 934P were potentially applicable enhancers for RTX absorption, which could be utilized in the oral delivery systems of RTX alone or in combination. This study provides referenced value for the research on oral delivery system of RTX.

4. Experimental

4.1. Materials

RTX was supplied by East China University of Science and Technology (Shanghai, China). Phenol Red (PR) was purchased from Kelong Reagent Co., Ltd. (Chengdu, China). Folic acid and pantoprazole were obtained from Sigma-Aldrich, Inc. (St. Louis, MO, USA). Cap-Na was provided by TCI (Shanghai) Development Co., Ltd. (Shanghai, China). Deo-Na was obtained from Sinopharm Chemical Reagent Co., Ltd. (Shanghai, China). Carbomer 934P was purchased from Shanghai Cansepec Scientific Instruments Co., Ltd. (Shanghai, China). Probenecid was obtained from Alfa Aesar (Tianjin) Chemicals Co., Ltd. (Tianjin, China). Verapamil was provided by Coben Pharmaceutical Co., Ltd. (Hangzhou, China). All other reagents were of at least analytical grade.

Dulbecco's Modified Eagle Medium (DMEM) was obtained from Thermo-Fisher Biochemical Products (Beijing) Co., Ltd. (Beijing, China). Fetal bovine serum (FBS) and non-essential amino acids solution were purchased from Hyclone Laboratories, Inc. (Logan, Utah, USA). Trypsin (1:250), HEPES and MTT were purchased from Sigma-Aldrich, Inc. (St. Louis, MO, USA). Moreover, 12-well Transwell insert (pore size of 0.4 μm, 1.12 cm^2, polycarbonate filter, Costar 3460) and plate were obtained by Corning Inc. (NY, USA).

Caco-2 cells were provided by Cell Biology Institution of Chinese Academy of Science (Shanghai, China). Wistar rats were obtained from the West China Laboratory Animal Center of Sichuan University (Chengdu, China).

4.2. In vitro transport studies of RTX in the Caco-2 cell monolayer model

4.2.1. Caco-2 cell culture

Caco-2 cells (passage of 46^{th}-55^{th}) were seeded in collagen coated Transwell insert at a density of 80,000 cells/cm^2 and cultured for 21 days prior to the transport experiments. The formation of confluent monolayers and tight junctions was confirmed by a transepithelial electrical resistance (TEER) value of above 300–500 Ω cm^2 and an apparent permeability coefficient (P_{app}) value of less than 10^{-6} cm/s for Flu-Na (Li et al. 2008), a hydrophilic marker primarily transported via paracellular pathway. TEER test was performed using a Millicell ERS Volt-Ohm Meter (Millipore, Bedford, MA, USA).

4.2.2. Bi-directional transport of RTX

The TEER values across the Caco-2 cell monolayer after 21 days cultivation were above 800 Ω cm^2 and the P_{app} values of Flu-Na were less than 10^{-7} cm/s, suggesting the formation of confluent monolayers. To begin the transport experiment, cells were rinsed with Hanks' Balanced Salt Solution (HBSS) containing 25 mM HEPES at pH 7.4 for three times, and the chambers were equilibrated with different transport buffers (apical chamber: HBSS without Ca^{2+}/Mg^{2+}; basolateral chamber: HBSS with Ca^{2+}/Mg^{2+}) for 30 min. In order to investigate the RTX transport in the apical-to-basolateral direction, 0.5 mL test solution and 1.5 mL blank receiver solution were loaded at the apical side and basolateral side, respectively. The RTX concentration in the test solutions was 5, 15, 20, 30, 45 and 60 μg/mL, respectively. Aliquots of 0.1 mL samples were taken from receiver chambers at various time intervals (30, 60, 90, 120, 150 and 180 min), and the volume was substituted by 0.1 mL blank receiver solution. Similarly, to investigate the RTX transport in the basolateral-to-apical direction, 1.5 mL test solution containing 20 μg/mL RTX was added at the basolateral side, while 0.5 mL blank receiver solution was added at the apical side. The procedures of sampling and replacement were performed as described above. Transport studies were carried out at 37 °C in an atmosphere of 5% CO_2.

RTX concentrations in the transport samples were analyzed by a high-performance liquid chromatographic (HPLC) method. And the apparent permeability coefficient (P_{app}) was calculated using the following equation (Zhou et al. 2009):

$$\mathrm{Papp} = \frac{\mathrm{dC/dt} \times \mathrm{V}}{\mathrm{A} \times \mathrm{C0}}$$

where dC/dt (μg·$mL^{-1}s^{-1}$) is the change of the accumulated drug concentration in the receiver chamber over time, V (mL) is the volume of the receiver compartment (1.5 mL), A (cm^2) represents the membrane surface area of Caco-2 monolayer (1.12 cm^2), and C_0 (μg/mL) is the initial RTX concentration in the donor chamber. All reported values were expressed as mean ± SD (n = 3).

4.2.3. *Effects of folic acid and ABC transporter inhibitors on the bi-directional transport of RTX*

Folic acid was selected as a competitive inhibitor of RTX absorption. Verapamil, probenecid and pantoprazole were utilized as P-gp, MRP and BCRP inhibitors, respectively. Their effects on the transport of RTX in both directions were investigated. Test solutions containing 20 μg/mL RTX with or without the addition of 10 μg/mL folic acid, 2 mM verapamil, probenecid or pantoprazole were applied as donor solutions. Transport experiments in both direction were performed as the procedures described above.

4.2.4. *Effects of absorption enhancers on the transport of RTX*

In order to investigate the enhancement effects of absorption enhancers on the RTX transport, 0.5 mL test solution containing 30 μg/mL RTX with or without the addition of various concentrations of Cap-Na (0.1%, 0.125%, 0.15%, 0.25% and 0.5% w/v), Deo-Na (0.025%, 0.05%, 0.075%, 0.1% and 0.25% w/v) or Carbomer 934P (0.1%, 0.25%, 0.5%, 0.75% and 1% w/v) was loaded at the apical side, and 1.5 mL of blank receiver solution was loaded at the basolateral side. The procedures of sampling and replenishment were performed as described above. To evaluate the toxic effects of absorption enhancers, 0.1 mL samples were collected from the donor chambers at the end of the experiment, and the amount of protein released from the cells was measured with BCA method.
TEER values were also measured at the end of each transport experiment (3 h). Then the cells were gently washed with HBSS for three times and supplemented with complete medium. TEER measurements were repeated after a 24-h culture. The TEER values measured prior to the transport experiments (t = 0) were employed as the initial values and expressed as 100%. All subsequent TEER values were presented as a percentage of the initial value.

4.2.5. *Cytotoxicity tests of absorption enhancers on Caco-2 cells*

The cytotoxicity of absorption enhancers on Caco-2 cells was evaluated by MTT method. The Caco-2 cells were seeded onto a 96-well plate at a density of 10,000 cells/well and cultured at 37 °C for 36 h. After the culture medium was aspirated, the cells were exposed to 100 μL test solution containing 30 μg/mL RTX with or without the addition tested concentrations of Cap-Na, Deo-Na or Carbomer 934P. Blank HBSS was taken as negative control. The 96-well plate was incubated at 37 °C for 3 h. Then the test solutions were removed, and the cells were rinsed by HBSS. Subsequently, 20 μL MTT (5 mg/mL) solution and 200 μL FBS-free DMEM were added to each well. After another 4-h incubation, the solution in each well was replaced by 200 μL of DMSO. The absorbance at a wavelength of 490 nm was then measured with varioskan@Flash instrument (Thermo Scientific, Waltham, MA, USA). The cytotoxicity of each compound was calculated as the percentage of the absorbance relative to that of the negative control.

4.3. *Rat in situ intestinal absorption studies of RTX*

4.3.1. *Animals*

Male Wistar rats (200–250 g) were provided by the West China Laboratory Animal Center of Sichuan University (Chengdu, China). Animal experiments were performed in accordance with the Guidelines for Animal Experimentation Sichuan University (Chengdu, China), and animal protocols were approved by the Animal Ethics Committee. Prior to the experiments, rats were housed in a temperature and humidity controlled room with free access to water and standard rat chow. The rats were starved overnight with free access to water before the surgery.

4.3.2. *Intestinal absorption of RTX in rat in situ intestinal recirculating perfusion model*

Absorption experiments were performed through the *in situ* intestine recirculating perfusion model according to the previously reported method (Li et al. 2009; Zhou et al. 2010), and Krebs-Ringer (K-R) solution was used as a perfusion buffer. Prior of the perfusion experiment, the loss of drug from perfusates was demonstrated due to absorption but not to instability and adsorption. To begin the perfusion experiment, rats were anaesthetized with 20% urethane (1 g/kg) intraperitoneally. The desired intestine from the duodenum to ileum was exposed through a midline abdominal incision. A small incision was made at the proximal duodenum and terminal ileum to allow washing of the intestinal luminal contents with pre-warmed normal saline (37 °C). Then the intestinal segment was cannulated with two polyethylene tubes, and the tubes were attached to a peristaltic pump and a glass vial to form a closed loop system. The entire system was rinsed with test solution (37 °C) at a constant flow rate of 5 mL/min with the peristaltic pump for approximately 10 min until the effluent perfusates were clear. Subsequently, 100 mL test solution (37 °C) was introduced into the loop, and the perfusion was conducted at a flow rate of 2.5 mL/min. The RTX concentration in test solution was 1.2, 2.4, 3.6, 4.8, 7.2 and 9.6 μg/mL, respectively. The entire surgical area was covered with a piece of sterilized absorbent gauze wetted with normal saline (37 °C). During the surgical process, the body temperature was maintained by a heat lamp. Each perfusion experiment lasted for 120 min, and 1 mL sample solution was replaced by equivalent fresh K-R solution at an interval of 15 min. At the end of the experiments, the animals were sacrificed, the segment between two cannulas was quickly excised without dragging, and its length was recorded.
In order to determine the volume change of perfusate in the intestinal perfusion experiment, PR (Ling et al. 2007) was added as non-absorbed marker in this study.

4.3.3. *Sample treatment and analysis*

Briefly, 0.5 mL collected sample was mixed with 1 mL methanol. Then the mixture was thoroughly vortexed and centrifuged at 12,000 rpm for 10 min. The supernatant was filtered through a 0.22-μm millipore membrane. A 20-μL filtrate was injected into HPLC system.
RTX and PR determination in the perfusion solution was performed by a HPLC method. And the amount of remaining RTX (X_t, μg) in each sample was determined. Then the effective permeability coefficient (P_{eff}, $cm \cdot s^{-1}$) was calculated using the following equation (Neerati et al. 2011):

$$\text{Peff} = \frac{dX/dt}{2\pi\ rLC0}$$

where dX/dt ($\mu g \cdot s^{-1}$) indicates the change of RTX amount in the perfusateover time. C_0 (μg/mL) is the initial RTX concentration in the perfusate and 2πrL is the diffusion area of the intestinal segment which is assumed to be a cylinder area.

4.3.4. Effects of folic acid and ABC transporter inhibitors on the intestinal absorption of RTX in rat in situ intestinal recirculating perfusion model

Test solutions containing 3.6 μg/mL RTX with or without the addition of 1.8 μg/mL folic acid, 2 mM verapamil, probenecid and pantoprazole were employed as perfusion solutions. The perfusion procedures were performed as described above.

4.3.5. Secretion of RTX from in situ intestine segments

After a tail vein injection of RTX (100 mg/kg), perfusion experiment was performed using blank K-R solution as the perfusate with or without bile duct ligation, respectively. P_{eff} values were calculated to assess the serection behavior of RTX from *in situ* small intestine segment.

4.3.6. Effects of absorption enhancers on the intestinal absorption of RTX in rat in situ single pass intestinal perfusion model

All operations until cannulation were performed as in the recirculating perfusion experiment. After cannulation, the proximal tube was attached to a peristaltic pump and a pre-weighed donor vial filled with test solutions successively, while the distal tube was linked into a pre-weighed receiver vial, and then a single pass intestinal perfusion (SPIP) system was formed (Jonker et al. 2002; Li et al. 2011). Prior to the experiment, the entire system was rinsed with test solution at a constant flow rate of 5 mL/min at 37 °C for approximately 10 min until the effluent perfusates were clear. Subsequently, the flow rate was adjusted to 0.25 mL/min, and the intestinal segment was perfused with test solution for about 30 min to achieve the absorption equilibrium and stable outflow rate. Test solution contained 4.8 μg/mL RTX with or without the addition of Cap-Na, Deo-Na or Carbomer 934P at various concentrations (0.25%, 0.5% and 1% w/v). The entire surgical area was covered with a piece of sterilized absorbent gauze wetted with normal saline (37 °C). During the surgical process, the body temperature was maintained by a heat lamp. Each perfusion experiment lasted for 120 min, and the donor vial and receiver vial were replaced with new ones at an interval of 15 min. At the end of the experiments, the animals were sacrificed, the segment between two cannulas was quickly excised without dragging, and its length was recorded.
The procedures of sample treatment and determination were performed as described in section 4.3.3. The perfusate volume correction was carried out by a gravimetric method. Volume of the influent and effluent perfusates was calculated according to the following equations:

$$Q_{in} = m_{in}/\rho_{in}, \quad Q_{out} = m_{out}/\rho_{out}$$

where Q_{in}, Q_{out}, m_{in}, m_{out}, ρ_{in} and ρ_{out} are the volume (mL), quality (g) and density (g/mL) of the influent and effluent perfusates, respectively. The densities of the influent and effluent perfusates were determined by weighing the contents of a known volume of perfusates using an electronic weighing balance.
The effective permeability coefficients (P_{eff}, cm/s) were calculated using following equations (Li et al. 2011):

$$P_{eff} = \frac{-Q \times \ln\left[(C_{out} \times Q_{out})/(C_{in} \times Q_{in})\right]}{2\pi r L}$$

where Q is the inflow rate (mL/min), C_{in} and C_{out} are the concentrations of RTX in the influent and effluent perfusates, t is the perfusion time (2 h), r is the radius of the intestinal segment (set as 0.2 cm), L is the length of the intestinal segment, and 2πrL is the diffusion area of the intestinal segment which is assumed to be a cylinder area.

4.3.7. Protein-release measurement

In order to measure the cumulative amount of protein released from the rat intestinal epithelium during the *in situ* SPIP experiments, 0.1 mL of samples were collected from the effluent perfusates at each time point and then mixed. The amount of released protein was determined by the modified BCA method using BSA as a standard. Blank K-R solution was used as a negative control. The relative protein-release ratios were expressed as folds of the amount of released protein caused by absorption enhancers relative to that of the negative control.

4.3.8. Histological evaluation of intestinal segments

At the end of the *in situ* SPIP experiments, the intestine was rapidly removed from the anesthetized rats and randomly cut into 3-cm segments from duodenum, jejunum and ileum, respectively. The tissue was made into slice through fixation, dehydration, embedding and dyeing serially. All slices were observed and photoed with Zeiss LSM510 Confocal Microscopy system (Carl Zeiss Co., Germany). To describe possible changes in the tissue structure during the experiment, following parameters (Sharma at al. 2005) were determined:
Nudeo-apical distance (NPA): measurement of the distance between the nucleus and apical membrane in enterocytes with a micrometer.
Villus index (V_i): measurement of the height (villi) and full width at half maximum (Width $_{1/2}$) with a micrometer. The index was calculated according to the equation:

$$V_i = Height/Width_{1/2}$$

Morphological scoring: evaluation of the morphological conditions of segments, including epithelial integrity, thickness, villus oedema and height. A scale from 0 to 4 was introduced, where 0 represents a normal undamaged segment and 4 indicates the severe damage on segment.
Five villus were randomly selected from each segment, and each villus was measured for five times.

4.4. Fitting kinetic models to concentration-time data of RTX

Three kinetic models were fitted to the concentration–time data of RTX obtained from *in vitro* and *in situ* absorption experiments. The first model assumes a passive absorption mechanism, the second corresponds to an active Michaelis-Menten process, and the third one is a combination of an active Michaelis-Menten and a passive mechanism. These models were described as following equations (Fernandez-Teruel et al. 2005):
Passive diffusion: $\frac{dC}{dt} = Ka \times C$
Active transport: $\frac{dC}{dt} = \frac{Vm \times C}{Km + C}$
Combination of passive and active transport:
$\frac{dC}{dt} = Ka \times C + \frac{Vm \times C}{Km + C}$
where K_a represents the passive absorption rate coefficient. V_m indicates the maximum transport rate and K_m is the Michaelis-Menten constant (the concentration of substrate at which the transport rate is $V_m/2$).
The fitting procedures were performed through Nonlinear Curve Fit and the goodness of fit was evaluated by and R^2 and SSE (Jaymin and Shah 1996).

4.5. Effects of absorption enhancers and ABC transporter inhibitors on oral bioavailability of RTX in rats

The oral bioavailability of RTX was studied in male Wistar rats (200 ± 20 g). The animals were fasted overnight prior to drug administration, with free access to water. Test solutions

contained 10 mg/ml RTX with or without addition of the absorption enhancers (Cap-Na, Deo-Na and Carbomer 934P at 0.25%, 0.5% and 1% g/mL, respectively) and transporter inhibitors (2 mM probenecid and pantoprazole) which were demonstrated effective *in vitro* and *in situ*. All animals received intragastric administration of test solution at a RTX dose of 100 mg/kg. Blood samples (0.25 ml) were withdrawn at 5, 30, 60, 120, 180, 240, 360, 480, 600 and 1440 min post-dosing from the retro-obital plexus. Serum (100 μl) was obtained by centrifuging at 4000 rpm for 10 min. Samples were stored at −20 °C until HPLC analysis.The collected samples were mixed with 200 μl methanol. Then the mixture was thoroughly vortexed and centrifuged at 12,000 rpm for 10 min. The supernatant was filtered through a 0.22-μm millipore membrane. A 20-μL filtrate was injected into HPLC system.

Pharmacokinetic parameters were calculated using Drug and Statistics Software (DAS 2.0; Mathematical Pharmacology Professional Committee of China). The plasma RTX concentration versus time curves were used to determine maximum plasma concentration (C_{max}), time to achieve maximum plasma concentration (T_{max}) and area under the concentration-time curve to the final sampling point ($AUC_{0\text{-}24}$).

4.6. Statistical analysis

The statistical analysis of the samples was performed using a Student's t-test with P-values < 0.05 as the minimal level of significance.

Acknowledgment: This research was supported by a grant from a scientific and technological support project of Sichuan Province, China.

References

Assaraf YG (2006) The role of multidrug resistance efflux transporters in antifolate resistance and folate homeostasis. Drug Resist Updat 9: 227–246.

Aùngst BJ (2000) Intestinal Permeation Enhancers. J Pharm Sci 89: 429–442.

Bansal T, Mishra G, Jaggi M, Khar RK, Talegaonkar S (2009) Effect of P-glycoprotein inhibitor, verapamil, on oral bioavailability and pharmacokinetics of irinotecan in rats. Eur J Pharm Sci 36: 580–590.

Borchard G, Luessen HL, Verhoef JC, Lehr CM, Junginger HE (1996) The potential of mucoadhesive polymers in enhancing intestinal peptide drug absorption. III: Effects of chitosan-glutamate and carbomer on epithelial tight junctions *in vitro*. J Control Release 39: 131–138.

Breedveld P, Beijnen JH, Schellens JHM (2006) Use of P-glycoprotein and BCRP inhibitors to improve oral bioavailability and CNS penetration of anticancer drugs. Trends Pharmacol Sci 27: 17–24.

Cercos-Fortea T, Casabo VG, Nacher A, Cejudo-Ferragud E, Polache A, Merino M (1997) Evidence of competitive inhibition of methotrexate absorption by leucovorin calcium in rat small intestine. Int J Pharm 155: 109–119.

Clarke SJ, Beale PJ, Rivory LP (2000) Clinical and preclinical pharmacokinetics of raltitrexed. Clin Pharmacokinet 39: 429–443.

Fernandez-Teruel C, Gonzalez-Alvarez I, Casabó VG, Ruiz-Garcia A, Bermejo M (2005) Kinetic modelling of the intestinal transport of sarafloxacin. Studies *in situ* in rat and *in vitro* in Caco-2 cells. J Drug Target 13:199–212.

Gao Y, He L, Katsumi H, Sakane T, Fujita T, Yamamoto A (2008) Improvement of intestinal absorption of water-soluble macromolecules by various polyamines: Intestinal mucosal toxicity and absorption-enhancing mechanism of spermine. Int J Pharm 354: 126–134.

Hamid KA, Katsumi H, Sakane T, Yamamoto A (2009) The effects of common solubilizing agents on the intestinal membrane barrier functions and membrane toxicity in rats. Int J Pharm 379: 100–108.

Huang CR, Wang GJ, Wu XL, Li H, Xie HT, Lv H, Sun JG (2006) Absorption enhancement study of astragaloside IV based on its transport mechanism in Caco-2 cells. Eur J Drug Metab Pharmacokinet 31: 5–10.

Jaymin, Shah (1996) Application of kinetic model to *in vitro* percutaneous permeation of drugs. Int J Pharm 133: 179–189.

Jodrell DI, Newell DR, Gibson W, Hughes LR, Calvert AH (1991) The pharmacokinetics of the quinazoline antifolate ICI D 1694 in mice and rats. Cancer Chemother Pharmacol 28: 331–338.

Jonker C, Hamman JH, Kotze AF (2002) Intestinal paracellular permeation enhancement with quaternised chitosan: *in situ* and *in vitro* evaluation. Int J Pharm 238: 205–213.

Junginger HE, Verhoef JC (1998) Macromolecules as safe penetration enhancers for hydrophilic drugs – a fiction? Pharm Sci Technol Today 9: 370–376.

Kurasawa M, Kuroda S, Kida N, Murata M, Oba A, Yamamoto T, Sasaki H (2009) Regulation of tight junction permeability by sodium caprate in human keratinocytes and reconstructed epidermis. Biochem Biophys Res Commun 381: 171–175.

LeCluyse EL, Sutton SC (1997) *In vitro* models for selection of development candidates. Permeability studies to define mechanisms of absorption enhancement. Adv Drug Deliv Rev 23: 163–183.

Lehr CM, Bouwstra JA, Kok W, De Boer AJ, Tukker JJ, Verhoef JC, Breimer DD, Junginger HE (1992) Effects of the mucoadhesive polymer polycarbophil on the intestinal absorption of a peptide drug in the rat. J Pharm Pharmacol 44: 402–407.

Lennernas H (1998) Human intestinal permeability. J Pharm Sci 87:403–410.

Leone-Bay A, Paton DR, Weidner JJ (2000) The development of delivery agents that facilitate the oral absorption of macromolecular drugs. Med Res Rev 20: 169–186.

Leslie EM, Deeley RG, Cole SP (2005) Multidrug resistance proteins: role of P-glycoprotein, MRP1, MRP2, and BCRP (ABCG2) in tissue defense. Toxicol Appl Pharmacol 204: 216–237.

Li C, Wainhaus S, Uss AS, Cheng KC (2008) High-Throughput Screening Using Caco-2 Cell and PAMPA Systems. In: Ehrhardt C, Kim KJ (eds) Drug Absorption Studies: *In Situ*, *In Vitro* and In Silico Models, New York, pp. 418–429.

Li H, Zhao X, Ma Y, Zhai G, Li L, Lou H (2009) Enhancement of gastrointestinal absorption of quercetin by solid lipid nanoparticles. J Control Rel 133: 238–244.

Li M, Si L, Rabbaa AK, Yan F, Qiu J, Li G (2011) Excipients enhance intestinal absorption of ganciclovir by P-gp inhibition: assessed *in vitro* by everted gut sac and *in situ* by improved intestinal perfusion. Int J Pharm 403: 37–45.

Lin YJ, Shen WC (1991) Effects of deoxycholate on the transepithelial transport of soucrose and horseradish peroxidase in filter-grown Madin-Darby canine kidney (MDCK) cells. Pharm Res 8: 498–501.

Lindenberg M, Kopp S, Dressman JB (2004) Classification of orally administered drugs on the World Health Organization model list of essential medicines according to the biopharmaceutics classification system. Eur J Pharm Biopharm 58: 265–278.

Ling W, Rui LC, Hua JX (2007) *In situ* intestinal absorption behaviors of tanshinone IIA from its inclusion complex with hydroxypropyl-beta-cyclodextrin. Biol Pharm Bull 30: 1918–1922.

Lo YL, Huang JD (2000) Effects of sodium deoxycholate and sodium caprate on the transport of epirubicin in human intestinal epithelial Caco-2 cell layers and everted gut sacs of rats. Biochem Pharmacol 59: 665 –672.

Luessen HL, de Leeuw BJ, Langemeÿer MW, de Boer AB, Verhoef JC, Junginger HE (1996) Mucoadhesive polymers in peroral peptide drug delivery. VI. Carbomer and chitosan improve the intestinal absorption of the peptide drug buserelin in vivo. Pharm Res 13: 1668 –1672.

Maher S, Leonard TW, Jacobsend J, Brayden DJ (2009) Safety and efficacy of sodium caprate in promoting oral drug absorption: from *in vitro* to the clinic. Adv Drug Deliv Rev 61: 1427–1449.

Manegold C, Buchholz E, Kloeppel R, Kreisel C, Smith M (2002) Phase I dose-escalating study of raltitrexed ('Tomudex') and cisplatin in metastatic non-small cell lung cancer. Lung Cancer 36: 183 –189.

Michels J, Geldart T, Darby A, Craddock L, Iveson A, Richardson L, Iveson T (2006) The combination of raltitrexed (Tomudex) and mitomycin-C in the treatment of advanced colorectal cancer–a phase II study. Clin Oncol (R. Coll. Radiol) 18: 431–435.

Mori S, Matsuura A, Rama Prasad YV, Takada K (2004) Studies on the intestinal absorption of low molecular weight heparin using saturated fatty acids and their derivatives as an absorption enhancer in rats. Biol Pharm Bull 27: 418–421.

Nakamura J, Takamura R, Kimura T, Muranishi S, Sezaki H (1979) Enhancement effect of methylxanth ines on the intestinal absorption of poorly

absorbable dyes from the rat small intestine. Biochem Pharmacol 28: 2957–2960.

Neerati P, Ganji D, Bedada SK (2011) Study on *in situ* and in vivo absorption kinetics of phenytoin by modulating P-glycoprotein with verapamil in rats. Eur J Pharm Sci 44: 27–31.

Pitelka DR, Taggart BN, Hamamoto ST (1983) Effects of extracellular calcium depletion on membrane topography and occluding junctions of mammary epithelial cells in culture. J Cell Biol 96: 613–624.

Planting A, de Jong M, Jansen P, Kerrebijn J, Smith M, Verweij J (2005) Phase I study of concomitant chemoradiation with raltitrexed in locally advanced head and neck cancer. Eur J Cancer 41: 93–97.

Sharma P, Varma MV, Chawla HP, Panchagnula R (2005) Absorption enhancement, mechanistic and toxicity studies of medium chain fatty acids, cyclodextrins and bile salts as peroral absorption enhancers. Farmaco 60: 884–893.

Sugibayashi K, Onuki Y, Takayama K (2009) Displacement of tight junction proteins from detergent-resistant membrane domains by treatment with sodium caprate. Eur J Pharm Sci 36: 246–253.

Thanou M, Verhoef JC, Nihot MT, Verheijden JH, Junginger HE (2001) Enhancement of the intestinal absorption of low molecular weight heparin (LMWH) in rats and pigs using Carbopol 934P. Pharm Res 18: 1638–1641.

Tomita M, Hayashi M, Horie T, Ishizawa T, Awazu S (1988) Enhancement of colonic drug absorption by the transcellular permeation route. Pharm Res 5: 786–789.

Tomita M, Sawada T, Ogawa T, Ouchi H, Hayashi M, Awazu S (1992) Differences in the enhancing effects of sodium caprate on colonic and jejunal drug absorption. Pharm Res 9: 648–653.

Van Cutsem E, Cunningham D, Maroun J, Cervantes A, Glimelius B (2002) Raltitrexed: current clinical status and future directions. Ann Oncol 13: 513–522.

Wang D, Gao Y, Yun L (2006) Study on brain targeting of raltitrexed following intranasal administration in rats. Cancer Chemother Pharmacol 57: 97–104.

Wang L, Tang X (2008) A novel ketoconazole bioadhesive effervescent tablet for vaginal delivery: design, *in vitro* and 'in vivo' evaluation. Int J Pharm 28:181–187.

Woods B, Paracha N, Scott DA, Thatcher N (2012) Raltitrexed plus cisplatin is cost-effective compared with pemetrexed plus cisplatin in patients with malignant pleural mesothelioma. Lung Cancer 75: 261–267.

Yasuno T, Okamoto H, Nagai M, Kimura S, Yamamoto T, Nagano K, Furubayashi T, Yoshikawa Y, Yasui H, Katsumi H, Sakane T, Yamamoto A (2012) *In vitro* study on the transport of zinc across intestinal epithelial cells using Caco-2 monolayers and isolated rat intestinal membranes. Bio Pharm Bull 35: 588–593.

Zhou L, Chow MS, Zuo Z (2009) Effect of sodium caprate on the oral absorptions of danshensu and salvianolic acid B. Int J Pharm 379: 109–118.

Zhou Y, Li W, Ma S, Ping L, Yang Z (2010) Enhancement of intestinal absorption of akebia saponin D by borneol and probenecid *in situ* and *in vitro*. Environ Toxicol Pharmacol 29: 229–234.